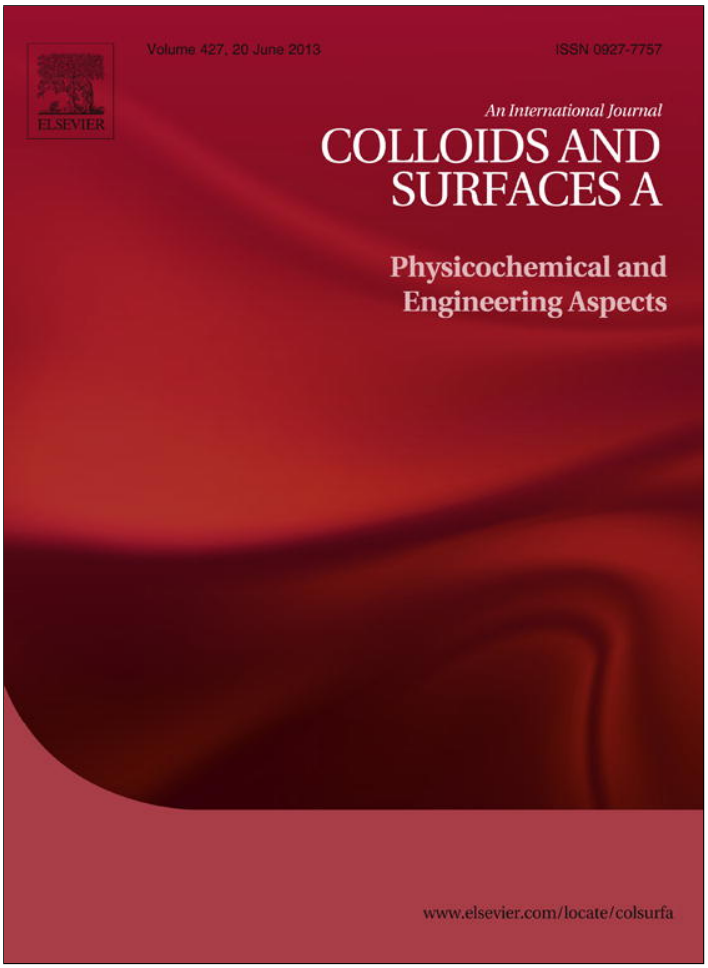

Colloids and Surfaces A: Physicochem. Eng. Aspects 427 (2013) 76–82

Contents lists available at SciVerse ScienceDirect

Colloids and Surfaces A: Physicochemical and Engineering Aspects

journal homepage: www.elsevier.com/locate/colsurfa

Aggregation kinetics of humic acids in the presence of calcium ions

Nanci Kloster[a], Maximiliano Brigante[b], Graciela Zanini[b], Marcelo Avena[b,*]

[a] EEA Anguil "Ing. Agr. Guillermo Covas", INTA, ruta Nac. N° 5 km 580, 6326 Anguil, La Pampa, Argentina
[b] INQUISUR-CONICET, Departamento de Química, Universidad Nacional del Sur, Av. Alem 1253, 8000 Bahía Blanca, Argentina

HIGHLIGHTS

- The aggregation rate of humic acid increases by increasing Ca^{2+} concentration.
- An aggregation mechanism is proposed.
- There is a fast Ca^{2+} binding followed by a slower attachment of molecules.
- Open fractal aggregate structures are observed.
- There is no fractionation of humics up to 60% of aggregation.

GRAPHICAL ABSTRACT

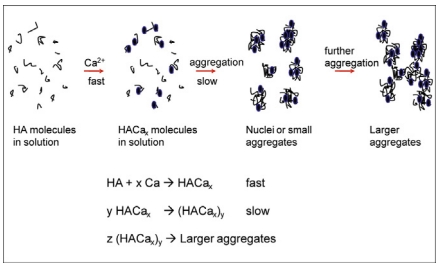

ARTICLE INFO

Article history:
Received 20 December 2012
Received in revised form 7 March 2013
Accepted 13 March 2013
Available online 22 March 2013

Keywords:
Coagulation kinetics
Humic substances
Aggregation mechanism
Flocculation

ABSTRACT

The aggregation kinetics of a humic acid (HA) sample as a function of Ca^{2+} concentration at pH 5, 7 and 9 was investigated. UV–VIS spectroscopy was employed to quantify the progress of the aggregation reaction, and electrophoresis was used to evaluate the zeta potential of the HA molecules. The aggregation rate increases significantly by increasing Ca^{2+} concentration at all investigated pH, being higher at pH 9 than at pH 5 and 7. An aggregation mechanism is proposed, which consists of at least two steps: a rapid binding of Ca^{2+} to humic molecules, followed by a slower process where HA molecules approach each other and become aggregated. This aggregation is possible because Ca^{2+} binding decreases the zeta potential of HA from −37 mV to −15 mV and because it is able to form bridges between HA molecules. There is no molecular fractionation up to 60% of aggregation. Above this value, HA aggregates become enriched with more aromatic HA molecules. The fast aggregation of HA in the presence of calcium ions implies that aggregates may temporarily trap, protect and transport pollutants in the environment.

1. Introduction

Humic substances (HS), such as humic acids (HA) and fulvic acids (FA), play relevant roles in the environment. They are very active in binding ions, organic molecules and solid surfaces and thereby affect significantly the soil structure, the mobility of organic contaminants and the bioavailability of metal ions. There are two main viewpoints regarding HS structure. According to relatively modern concepts, HS are regarded as a supramolecular assembly of small to large molecules [1,2], which form dynamic associations stabilized by hydrophobic interactions and hydrogen bonds [3]. The other, more traditional viewpoint, proposes that HS are relatively large polymeric molecules [4]. As indicated by Avena and Wilkinson [5], although these conceptual models may be still under discussion, supporters of both views agree that HA are able to form aggregates in aqueous media or in the solid state. These aggregates are stabilized by hydrophobic interactions, hydrogen bonds, and by the presence of metal ions, such as Ca(II), Fe(III) or Al(III) [6–8]. Therefore, characterization of HA is often focused on intermolecular interactions [9–11], factors that promote aggregation or disaggregation [12–14] and mechanisms of the aggregation–disaggregation processes [15,16].

The aggregation of HA is the result of molecular interactions that depend on environmental conditions such as pH, ionic strength, presence of multivalent metal ions, organic compounds and solid particles [11]. Aggregation in absence of cations is usually favoured

* Corresponding author. Tel.: +54 291 4595101x3579.
E-mail address: mavena@uns.edu.ar (M. Avena).

0927-7757/$ – see front matter © 2013 Elsevier B.V. All rights reserved.
http://dx.doi.org/10.1016/j.colsurfa.2013.03.030

by decreasing the solution pH because protonation of functional groups, mainly carboxylates and phenolates, leads to a decreased electrostatic repulsion among the molecules and to the formation of intermolecular H-bonds and other non-electrostatic interactions [17]. In the presence of multivalent cations aggregation is promoted via charge neutralization and cation bridge formation between different HA molecules [18]. Recent molecular dynamics simulations suggest that Ca^{2+} is mainly associated with carboxylic groups of natural organic matter molecules, forming bidentate complexes [19]. They show that calcium can direct affect aggregation by bridging carboxylic groups of different molecules, bringing and holding them together. In addition, calcium ions can also affect aggregation by coordinating simultaneously two carboxylic groups of the same HA molecule, which produces a calcium–HA complex with reduced net negative charge, thus allowing such complexes to approach each other and interact via hydrogen bonds [19].

The effects of cations on HA aggregation are usually pH dependent. In the case of Ca^{2+}, for example, Baloousha et al. [6] showed that at low pH 4.5, where the functional groups are weakly dissociated and the negative charge of HA is low, there is a small effect of Ca^{2+} concentration on HA aggregation. In contrast, at high pH 9.4, where most of the functional groups are dissociated and the negative charge is high, there is a significant effect of Ca^{2+} concentration on aggregation due to the important binding of Ca^{2+}.

There is increasing awareness that the kinetic properties of humic substances are very important in determining their reactivity in nature. Town et al. [20], for example, found that the size of humic entities may significantly affect their kinetics of metal binding. Yamashita et al. [21] recently investigated the deposition kinetics of HA in porous media. Equally important are the dynamics of aggregation. This is likely a significant environmental process, and its study will help to understand the aggregation mechanism and processes that control the transport of organic and inorganic pollutants in nature.

Even though HA aggregation studies have been reported in several publications, all of them deal mainly with aggregation under equilibrium or near equilibrium situations. No study has focused on the aggregation kinetics of HA. Therefore, the aim of this work is to study the aggregation kinetics of a HA sample under different conditions. The effects of pH and Ca^{2+} concentration were investigated in order to develop a simple aggregation mechanism and to gain insights into the dynamics of HA in the environment.

2. Materials and methods

The HA sample was obtained from an Argentinean agricultural soil classified as Entic Haplustoll. It was fractionated, purified and freeze-dried according to the procedure recommended by the International Humic Substances Society (IHSS) [22]. The C, H and N contents, determined with an Exeter CE 440 elemental analyzer, were 53.2%, 3.8% and 3.9% respectively.

In order to gain information on the electrostatic interaction between humic acid molecules, their zeta potential (ζ) under different conditions was measured with a Zetasizer ZS90 instrument (Malvern, UK). Three types of experiments were performed: (a) ζ vs. pH measurements at constant ionic strength, with either NaCl or $CaCl_2$ as the supporting electrolyte; (b) ζ vs. $CaCl_2$ concentration measurements at constant pH; and (c) ζ vs. time measurements at selected pH and $CaCl_2$ concentrations. For ζ vs. pH measurements, 50 mL of a 50 mg L^{-1} HA solution were placed in a reaction vessel with either NaCl or $CaCl_2$ (ionic strength, IS = 0.01), and the pH of the solution was adjusted to 10 with NaOH and equilibrated under continuous stirring (450 rpm). After ζ was measured, the pH was lowered by adding a small volume of HCl, and ζ was again measured after 10 min of equilibration. This procedure was repeated until the pH was 2. For ζ vs. $CaCl_2$ concentration measurements, aliquots of 10 mL of a 50 mg L^{-1} HA solution in 0.01 M NaCl and at the desired pH were placed in capped test tubes. Different volumes of a 0.6 M $CaCl_2$ solution were then added to the tubes in order to cover a Ca^{2+} concentration range from 0 to 3 mM. After 12 h of equilibration, the pH was checked to ensure that it was the same for all tubes before measurement of ζ. For ζ vs. time measurements, a 50 mg L^{-1} HA solution in 0.01 M NaCl was prepared at the desired pH and equilibrated. A desired volume of a 0.6 M $CaCl_2$ solution was then added to the system, and ζ was registered at different times during 1 h.

Aggregation kinetic experiments were carried out in a batch system using a cylindrical, temperature-controlled ($25 \pm 0.2\,^{\circ}C$) reaction vessel covered with a glass cap. Before starting the experiment, a stock 1000 mg L^{-1} HA solution was prepared by dissolving the solid HA at pH 10 in order to obtain a well-dissolved [6] and well-disaggregated [5] sample. A 50 mg L^{-1} HA solution was prepared in the reaction vessel by adding a measured volume of the stock solution to 50 mL of 0.01 M NaCl, which was used as the supporting electrolyte, and the pH was adjusted to the desired value with small additions of either NaOH or HCl.

The aggregation kinetic experiment was started by adding a known volume of a 0.6 M $CaCl_2$ solution to the reaction vessel in order to obtain Ca^{2+} concentrations of 0.3, 0.8, 1.2, 1.4, 1.6, 1.8, 2.4, and 3.2 mM. These concentrations are within the calcium concentration range of soil solutions from around the world [23]. Constant stirring (450 rpm) was maintained with a magnetic bar and an IKA RH KT/C magnetic stirrer. At different times (usually every 1 or 2 min during the first 15 min of reaction and every 10 min afterwards), an aliquot of the solution was withdrawn, gently filtered with a 0.45 μm pore size membrane in order to separate the aggregates from the supernatant, and the HA that remained in solution was quantified by taking a spectrum in the 200–900 nm wavelength range with an Agilent 8453 UV–VIS diode array spectrophotometer equipped with a Hellma 1 cm quartz cell. Calibration curves at the working pH were constructed with several HA solutions (concentration range between 2 mg L^{-1} and 60 mg L^{-1}) prepared from the stock solution.

The aggregation kinetics was evaluated by plotting the degree of progress of the aggregation reaction, α, as a function of time (t). α is defined as

$$\alpha = \frac{C_0 - C}{C_0} \quad (1)$$

where C_0 is the initial HA concentration (which is also the total HA concentration in the experiment) and C is the HA concentration that remains in solution (measured spectrophotometrically) at a certain reaction time. A value $\alpha = 0$ means 0% aggregation and $\alpha = 1$ means 100% aggregation. An α vs. t curve is called an aggregation kinetic curve.

The formation of HA aggregates was also followed by optical microscopy. A 50 mg L^{-1} HA solution at pH 7 and containing 4 mM Ca^{2+} was observed with a HOKENN optical microscope equipped with a HOKENN Micro Image Analysis Software.

3. Results and discussion

Fig. 1 shows the zeta potential of the HA sample under different conditions. The effects of pH in NaCl and $CaCl_2$ solutions are shown in Fig. 1a. ζ is negative at all pH values in both electrolytes. In NaCl, ζ is −20 mV at pH 2, decreases until −37 mV at pH 5 and then remains nearly constant up to pH 10. The behaviour is nearly coincident with that reported by Hosse and Wilkinson [24] for two HA samples. The decrease in ζ from pH 2 to 5 results from deprotonation of mainly carboxylic groups [17,24], that generates negative charges in the HA molecules. Although the molecules suffer further deprotonation at higher pH due to the presence of other ionizable

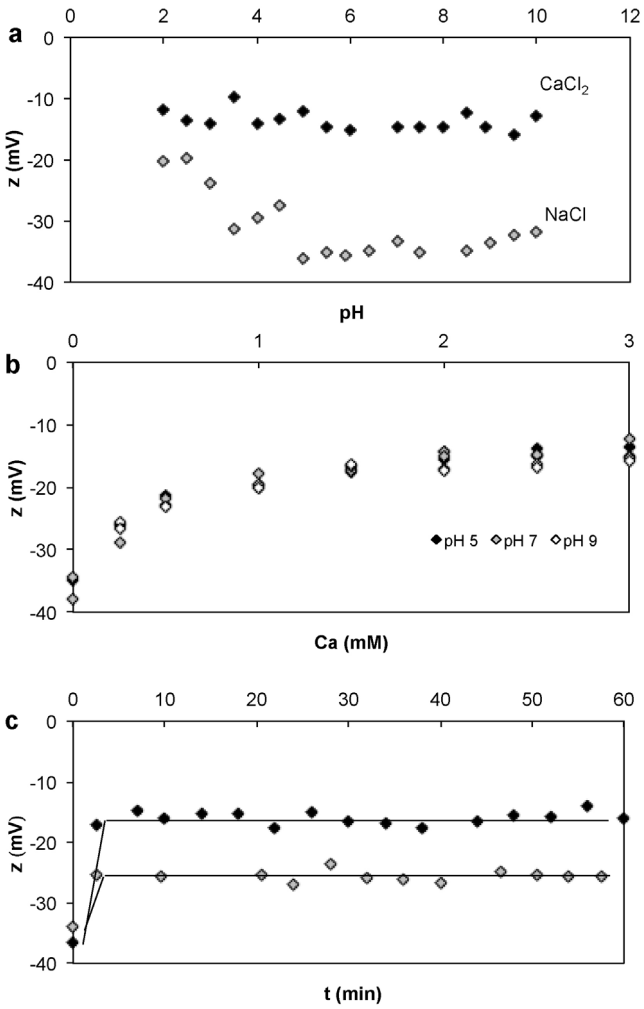

Fig. 1. (a) ζ of HA in 10 mM NaCl and 3 mM $CaCl_2$; (b) influence of Ca^{2+} concentration on ζ at different pH; (c) effect of time on ζ after changing Ca^{2+} concentration from 0 to 0.8 mM (grey symbols) or to 2 mM (black symbols). Data at $t = 0$ correspond to the value of ζ in 10 mM NaCl, before addition of Ca^{2+}. Lines are drawn as a visual guide.

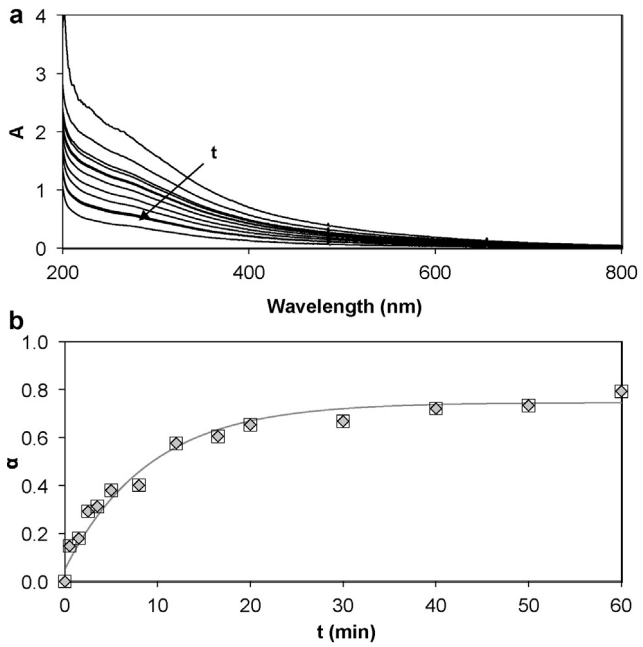

Fig. 2. (a) UV–VIS spectra of the supernatant of a HA solution during a kinetic experiment at pH 5 and Ca^{2+} concentration 1.6 mM. Each spectrum corresponds to a different sampling time. The arrow with the *t* symbol indicates increasing sampling times of 0, 0.5, 2, 2.5, 3.5, 5.5, 8, 12, 16.5, 20, 30, 40, 50 and 60 min. (b) Aggregation kinetic curve resulting from the above spectra. The line is the best fit calculated by Eq. (4) and parameters in Table 1.

groups, such as phenolic groups, ζ does not change significantly at high pH because ζ becomes rather insensitive to increasing charge at high charge densities [25]. In $CaCl_2$, ζ is always less negative than in NaCl and remains at around −15 mV at all studied pH values. The different ζ values in $CaCl_2$ as compared to those in NaCl are the result of Ca^{2+} binding to HA molecules, which has been demonstrated in many publications [26,27]. The effects of varying Ca^{2+} concentration at pH 5, 7 and 9 are shown in Fig. 1b. The behaviour is independent of pH, and in all cases ζ is around −37 mV in the absence of Ca^{2+} and becomes less negative as Ca^{2+} concentration increases. The effects are rather significant up to 1 mM Ca^{2+} concentration, where ζ is −19 mV. Above this concentration changes are smaller, and ζ reaches a value of −15 mV at 3 mM Ca^{2+}. Although Ca^{2+} binding decreases the net negative charge of the molecules, making the value of ζ less negative, it is clear that the binding is not able to produce charge reversal at any studied pH. Results are similar to those shown by Majzik and Tombácz [28] for zeta potential of a HA at varying Ca^{2+} concentration and pH 6.5. They are also in agreement with potentiometric measurements of Ca^{2+} binding to humic substances combined with calculations performed with the NICA-Donnan model, which show that the specific binding of Ca^{2+} to functional groups of the molecules plus the nonspecific binding due to electrostatic attraction of the cation by the negatively charged HA molecules do not produce charge reversal in humics [26,27,29].

Fig. 1c shows the variation of ζ with time after Ca^{2+} addition. ζ is already stabilized at its equilibrium value after 2 min of reaction, which is the shortest time that could be explored in this kind of experiments. The constancy in ζ indicates that Ca^{2+} binding to the humic, takes place in less than 2 min, which will be considered to be a fast process in comparison with the slower aggregation process (see below). This behaviour is in agreement with the results of Town et al. [20], who showed that for rapidly dehydrating metal ions such as $Cu(OH_2)_6^{2+}$, which is also the case of aqueous Ca^{2+} ions, the binding is very fast.

Fig. 2a shows the changes in the UV–VIS spectra of the supernatant solution during a representative aggregation kinetic experiment, where each spectrum corresponds to a different sampling time. Fig. 2b, in addition, shows the aggregation kinetic curve resulting from these spectra. The absorbance at any wavelength decreases with time, indicating a decrease in the concentration of dissolved HA, and therefore increasing aggregation. The aggregation kinetic curve shows that aggregation takes place mainly in the first 15–20 min of reaction and that the curve levels off at longer times. Not all HA molecules become aggregated during the reaction time ($\alpha < 1$ after 60 min of reaction).

Aggregation kinetic curves obtained at pH 5 at different Ca^{2+} concentrations are shown in Fig. 3. A large effect of Ca^{2+} concentration is observed. In 0.8 mM Ca^{2+} the aggregation is insignificant, but at higher Ca^{2+} concentrations aggregation readily takes place and increases as Ca^{2+} concentration increases.

Kinetic data as those shown in Fig. 3 were analyzed in terms of the following first-order rate equation [30]:

$$R = -\frac{dC}{dt} = k(C - C_f) \quad (2)$$

where R is the aggregation rate, k is the rate constant and C_f is the final concentration of dissolved HA after long reaction times, i.e.,

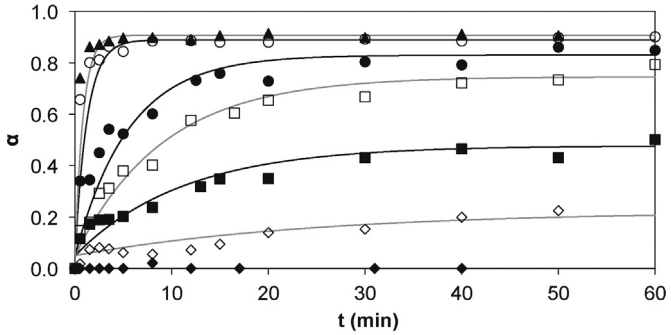

Fig. 3. Aggregation kinetic curves of HA at pH 5 at different Ca^{2+} concentrations: 0.8 mM (♦), 1.2 mM (◊), 1.4 mM (■), 1.6 mM (□), 1.8 mM (●), 2.4 mM (○) and 3.2 mM (▲). Lines are the best fit calculated by Eq. (4) and parameters in Table 1.

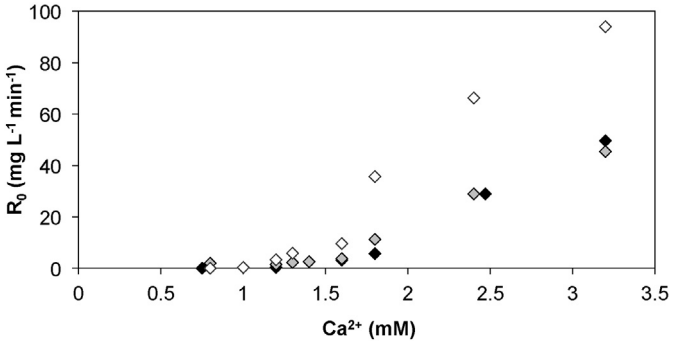

Fig. 4. Influence of Ca^{2+} concentration on the initial aggregation rate at pH 5 (♦), 7 (◇) and 9 (◊).

the concentration of HA that remains dissolved after reaching the plateau of the aggregation curve. Integration of Eq. (2) leads to:

$$C = C_f + (C_0 - C_f)e^{-kt} \quad (3)$$

or, in terms of α

$$\alpha = \alpha_f - \alpha_f e^{-kt} \quad (4)$$

where $\alpha_f = (C_0 - C_f)/C_0$, i.e., the value of α after reaching the plateau of the curve. The rate constant k can be easily calculated by fitting the curves with Eq. (4), and once k is known, the initial aggregation rate, R_0, can be calculated from

$$R_0 = k(C_0 - C_f) = kC_0\alpha_f \quad (5)$$

which comes directly from Eq. (2) under the condition $C = C_0$ at $t = 0$. The use of these equations does not intend to prove a certain aggregation mechanism. However, this procedure allows calculating the initial aggregation rate with parameters that were obtained by fitting all data points of an aggregation curve, overcoming the problems of estimating the initial slope of a curve with just the first data points.

Calculations with Eq. (4) are shown as lines in Figs. 2 and 3, and the corresponding parameters (k and α_f) and R_0 values are listed in Table 1.

The effects of Ca^{2+} concentration on the initial aggregation rate are plotted in Fig. 4 for the three pH values studied. The minimum concentration needed to produce aggregation was between 0.8 and 1.2 mM (as better seen in Table 1). Therefore, a value of 1.0 ± 0.2 mM can be recognized as a critical aggregation concentration or critical coagulation concentration (CCC) value for the studied HA. Although not using kinetic experiments, Wall and Chopin [31] found a similar critical concentration for the coagulation of a purified Aldrich HA with Ca^{2+} cations at pH 8.3, and Hong and Elimelech [32] found that natural organic matter coagulated above 1 mM Ca^{2+} at pH between 4 and 8.

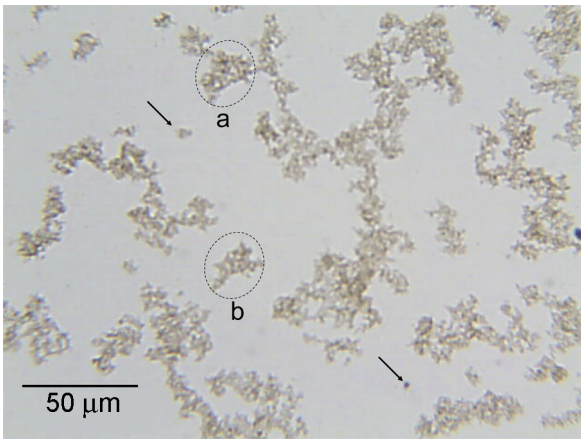

Fig. 5. Optical microphotograph of HA aggregates formed after 60 min. Circle (a) shows a subunit forming part of a large Y-shape aggregate. Circle (b) shows a similar but freely moving subunit. These subunits are made from smaller (1–5 μm) aggregates. Two of these small aggregates are indicated by the arrows. HA concentration: 50 mg L^{-1}; Ca^{2+} concentration: 4 mM; pH: 7.

Fig. 4 also shows that above the CCC the aggregation rate increases with increasing Ca^{2+} concentration. The effect of Ca^{2+} concentration on R_0 is rather similar at pH 5 and 7, but is more marked at pH 9.

Fig. 5 shows an optical microphotograph of the HA aggregates produced at pH 7 and 4 mM Ca^{2+} concentration after long aggregation times. Open aggregate structures are observed. The figure shows, for example, a large (around 100 μm) Y-shape aggregate, which is composed of smaller subunits of 20–30 μm size. Two of

Table 1
Kinetic parameters.

Ca^{2+} (mM)	pH 5			pH 7			pH 9		
	α_f	k[a]	R_0[a]	α_f	k	R_0	α_f	k	R_0
0.3	–[b]	–	–	0	0	0	–	–	–
0.8	0	0	0	0.01	0.05	0.03	0.06	0.03	0.10
1.0	–	–	–	–	–	–	0.17	0.05	0.40
1.2	0.16	0.04	0.30	0.20	0.09	0.90	0.58	0.12	3.40
1.3	–	–	–	0.50	0.09	2.20	0.66	0.20	5.90
1.4	0.43	0.09	1.90	0.63	0.09	2.60	–	–	–
1.6	0.70	0.11	3.30	0.68	0.13	3.80	0.74	0.28	9.60
1.8	0.78	0.18	7.00	0.74	0.35	11.20	0.85	0.90	35.70
2.4	0.84	0.80	31.20	0.84	0.80	28.90	0.89	1.60	66.30
3.2	0.86	1.20	46.60	0.87	1.10	45.50	0.92	2.10	94.00

[a] Units of k: min^{-1}; units of R_0: mg L^{-1} min^{-1}.
[b] (–) not measured.

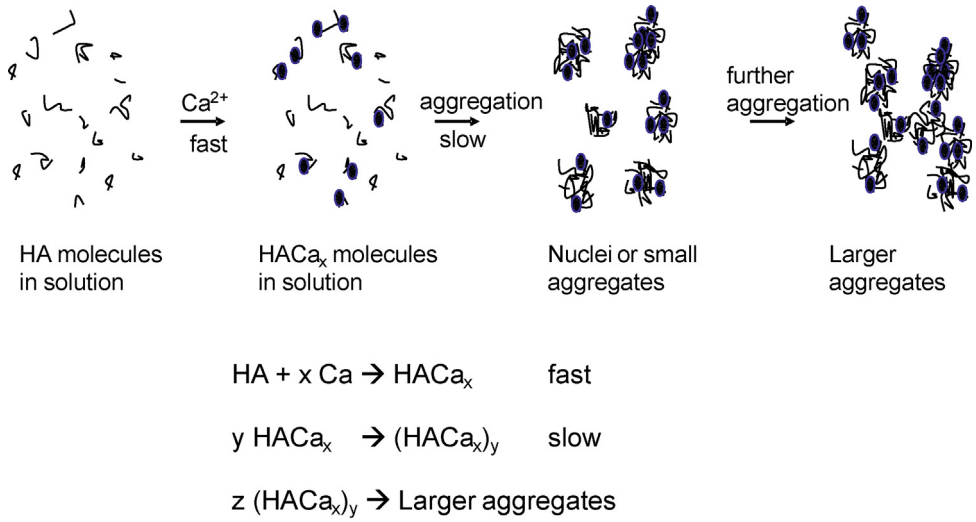

Fig. 6. Schematic representation of the steps involved in the HA aggregation process in the presence of Ca^{2+} ions (represented as spheres). Not to scale.

these subunits are marked in the figure, one of them (a) forming part of the Y-shape aggregate and another one (b) not forming part of it. In addition, these subunits seem to be composed of even smaller aggregates (two of them are indicated with arrows) of 1–5 μm size. The observation of the system with the microscope revealed that the subunits and the smaller aggregates were rather mobile, subject to Brownian motion, and that large structures like the Y-shape aggregate were continuously being formed and disrupted, with the subunits continuously entering or leaving the aggregates. The hierarchical architecture of the aggregates observed in Fig. 5 seems to be rather usual for humic acids [33], and the results obtained with the optical microscope complement findings obtained by other authors using higher magnifications. Baloousha et al. [6], for example, reported the presence of 1–5 μm aggregates of the Suwannee river humic acid (SRHA) in $CaCl_2$ solutions as observed by transmission electron microscopy. These authors made a thorough review and analysis of published data, and concluded that HA aggregates are formed by small basic units of less than 10 nm size, and that the size of aggregates is dependent on the pH and divalent cation concentration. They indicated that cations such as Ca^{2+} increased aggregation through the formation of intra- or intermolecular bridges between the negatively charged humic acid molecules.

Data presented so far indicates that the formation of HA aggregates from dissolved HA molecules in the presence of Ca^{2+} seems to be rather complicated. Processes such as Ca^{2+} binding to dissolved HA molecules, nucleation and growth of small aggregates, and aggregate-aggregate binding to produce even larger aggregates should be involved. A very simplified scheme of the process is drawn in Fig. 6. The initial and triggering step must be Ca^{2+} binding to dissolved HA molecules. This is fast, taking place in <2 min thus this is not the rate-determining step of the aggregation process. The formed $HACa_x$ molecules, where x represents in average the number of Ca^{2+} ions bound per HA molecule, become less negatively charged and they can form nuclei or small aggregates, with Ca^{2+} ions acting as intermolecular bridges. These nuclei or small aggregates can suffer further aggregation and thus larger aggregates are formed.

Since either the second or the third steps (Fig. 6) are slower than Ca^{2+} binding, they seem to be rate-determining, and thus the aggregation rate should depend on the efficiency of collisions among $HACa_x$ molecules or small aggregates. This efficiency can be understood in terms of a combination of long-range repulsive forces due to the negative ζ of the molecules and short-range binding forces due to the presence of Ca^{2+} in the molecules. If ζ is highly negative, there will be an important electrostatic barrier between approaching molecules or small aggregates and therefore collisions will be rather inefficient. This is the case at Ca^{2+} concentrations below 1 mM, where aggregation is insignificant. At Ca^{2+} concentrations equal or above 1 mM (CCC), ζ becomes less negative and therefore two approaching entities have more probability of becoming in close contact, allowing bound Ca^{2+} to act as a bridge between them. Under these conditions, collisions are more efficient and aggregation proceeds significantly. It is interesting to note that above the CCC the aggregation rate increases linearly with Ca^{2+} even though ζ remains nearly constant. Under these conditions, the increase in the collisions efficiency is mainly due to an increased amount of Ca^{2+} bound to HA rather than to a decrease in electrostatic repulsion between the approaching entities. The higher the number of Ca^{2+} bound per HA molecule, the higher the probability of formation of intermolecular Ca^{2+} bridges. A similar explanation could be given for the higher aggregation rate at pH 9 than at pH 5 or 7. ζ is independent of pH at all investigated Ca^{2+} concentrations, and thus the higher aggregation rates at pH 9 must be a consequence of higher Ca^{2+} binding to the humics at this pH.

It is nowadays quite accepted that HAs are a rather complex mixture of molecules, which may have different spectroscopic properties. The UV–VIS spectra shown in Fig. 7, therefore, represent the sum of the individual spectra of all HA components that remain in solution and unaggregated during an aggregation run. The ratio E2/E3 (ratio between absorbance of the HA solution at 250 nm and at 365 nm) gives information on the aromaticity of the

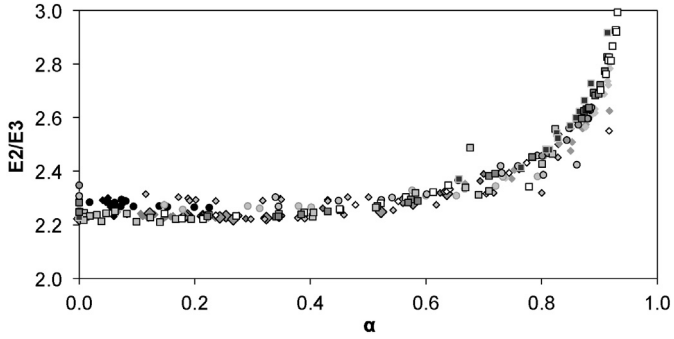

Fig. 7. E2/E3 vs. α for all conditions investigated.

HA, and is inversely correlated to aromaticity [34,35]; i.e., samples with low E2/E3 are rich in aromatic components and vice versa. It is then useful to evaluate the value of E2/E3 as aggregation proceeds, because information about humic acid fractionation during aggregation can be obtained. Fig. 7 shows the E2/E3 vs. α curves for all the experiments performed. Notably, all data points describe a unique curve indicating that the behaviour is the same under all the explored conditions. E2/E3 remains nearly constant and equal to the ratio E2/E3 of the original HA sample up to $\alpha \approx 0.6$ and then increases as α increases. This means that there is no fractionation (no preferential aggregation of some HA components) up to 60% of aggregation, but that above this value the aggregates become richer in aromatic components.

Unfortunately there are no data in the literature regarding E2/E3 values during aggregation of HA. There are data about fractionation upon adsorption on oxide particles under equilibrium conditions. Janot et al. [34], for example, found preferential adsorption of aromatic HA components on α-Al_2O_3 at pH 6.8, which, according to the authors is in agreement with other literature data. Kang and Xing [36], on the contrary, found the opposite effect for adsorption of a humic acid onto goethite. Our results on HA aggregation kinetics are different to both type of results on HA adsorption. Indeed, no preferential aggregation occurs, at least up to $\alpha \approx 0.6$, for which we have no conclusive explanation. Perhaps the presence of Ca^{2+} ions in our aggregating systems is a key factor to explain the observed behaviour. Even though HA is a complex mixture of molecules, all of them have at a certain extent ionizable groups capable of complexing Ca^{2+}, and therefore all of them have similar ability of forming intermolecular Ca^{2+} bridges and aggregate without preference. Further research is still needed in this respect.

4. Conclusions

The aggregation rate of HA increased significantly by increasing Ca^{2+} concentration in the pH range 5–9. The kinetic study allows postulating a reaction mechanism, where Ca^{2+} binding takes place rapidly, followed by a slower formation of nuclei or small aggregates of $HACa_x$ molecules. Further aggregation also takes place yielding the formation of large aggregates that can be observed by optical microscopy and even with the naked eye. Calcium binding to HA likely plays two key roles in the aggregation process: it decreases the repulsive forces between HA molecules by decreasing their zeta potential, and leads to the formation of calcium bridges between two approaching molecules.

A critical coagulation concentration of 1.0 ± 0.2 mM Ca^{2+} was found from kinetic data, which is similar to CCC values obtained by other authors from "equilibrium" coagulation studies. Thus, the presence of Ca^{2+} and perhaps other di- or trivalent cations in natural media is fundamental to maintain the stability of HA aggregates. The results presented above may have significant importance for environmental systems because they imply that at high calcium concentration, HA can quickly aggregate, and temporarily trap, protect and transport organic molecules, metal ions, pesticides and other pollutants. The dynamics of the HA aggregation–disaggregation processes should play an important role in the transport and protection of pollutants in the environment. Since it is known that the binding of polyvalent ions such as Ca^{2+} produces stabilization of soil organic matter, the results may be also important to understand carbon sequestration and storage in calcareous soils [7].

Acknowledgements

This research was financed by CONICET, ANPCYT, UNS and INTA. MB, GZ and MA are members of CONICET.

References

[1] V. D'Orazio, N. Senesi, Spectroscopic properties of humic acids isolated from the rizosphere and bulk soil compartments and fractionated by size exclusion chromatography, Soil Biol. Biochem. 41 (2009) 1775–1781.
[2] P. Conte, A. Piccolo, Conformational arrangement of dissolved humic substances. Influence of solution composition on association of humic molecules, Environ. Sci. Technol. 33 (1999) 1682–1690.
[3] R. Sutton, G. Sposito, Molecular structure in soil humic substances: the new view, Environ. Sci. Technol. 39 (2005) 9009–9015.
[4] R.S. Swift, Macromolecular properties of soil humic substances. Fact, fiction, and opinion, Soil Science 164 (1999) 790–802.
[5] M.J. Avena, K.J. Wilkinson, Disaggregation kinetic of a peat humic acid: mechanism and pH effects, Environ. Sci. Technol. 36 (2002) 5100–5105.
[6] M. Baloousha, M. Motelica-Heino, P. Le Coustumer, Conformation and size of humic substances: effects of major cation concentration and type, pH, salinity, and residence time, Colloids Surf., A 272 (2006) 48–55.
[7] D.C. Olk, A chemical fractionation for structure-function relations of soil organic matter in nutrient cycling, Soil Sci. Soc. Am. J. 70 (2006) 1013–1022.
[8] P. Zhou, H. Yan, B. Gu, Competitive complexation of metal ions with humic substances, Chemosphere 58 (2005) 1327–1337.
[9] G.E. Schaumann, S. Thiele-Bruhn, Molecular modeling of soil organic matter: squaring the circle, Geoderma 166 (2011) 1–14.
[10] M. Terashima, S. Tanaka, M. Fukushima, Coagulation characteristics of humic acid modified with glucosamine or taurine, Chemosphere 69 (2007) 240–246.
[11] E. Tombácz, Colloidal properties of humic acids and spontaneous changes of their colloidal state under variable solution conditions, Soil Science 164 (1999) 814–824.
[12] M. Pédrot, A. Dia, M. Davranche, Dynamic structure of humic substances: rare earth elements as a fingerprint, J. Colloid Interface Sci. 345 (2010) 206–213.
[13] M. Brigante, G. Zanini, M. Avena, Effects of pH, anions and cations on the dissolution kinetic of the humic acid particles, Colloids Surf., A 347 (2009) 180–186.
[14] I. Christl, R. Kretzschmar, C-1s NEXAFS spectroscopy reveals chemical fractionation of humic acid by cation-induced coagulation, Environ. Sci. Technol. 41 (2007) 1915–1920.
[15] J. Kučerík, M. Drastík, O. Zmeškal, A. Ctvrtníčková, Ultrasonic spectroscopy and fractal analysis in the study on progressive aggregation of humic substances in diluted solutions, WSEAS Transactions on Environment and Development 11 (2009) 705–715.
[16] M. Brigante, G. Zanini, M. Avena, On the dissolution kinetics of humic acid particles: effects of pH, temperature and Ca concentration, Colloids Surf., A 294 (2007) 64–70.
[17] R.A. Alvarez-Puebla, J.J. Garrido, Effect of pH on the aggregation of a gray humic acid in colloidal and solid states, Chemosphere 59 (2005) 659–667.
[18] E. Tipping, Cation Binding by Humic Substances, Cambridge University Press, Cambridge, New York, 2002.
[19] A.G. Kalinichev, E. Iskrenova-Tchoukova, W.Y. Ahn, M.M. Clark, R.J. Kirkpatrik, Effects of Ca^{2+} on supramolecular aggregation of natural organic matter in aqueous solutions: a comparison of molecular mmodeling approaches, Geoderma 169 (2011) 27–32.
[20] R.M. Town, H.P. van Leeuwen, J. Buffle, Chemodynamics of soft nanoparticulate complexes: Cu(II) and Ni(II) with fulvic acid and aquatic humic acids, Environ. Sci. Technol. 46 (2012) 10487–10498.
[21] Y. Yamashita, T. Tanaka, Y. Adachi, Transport behaviour and deposition kinetics of humic acids under acidic conditions in porous media, Colloids Surf., A 417 (2013) 230–235.
[22] R.S. Swift, Organic matter characterization. In: D.L. Sparks (Ed.), Methods of Soil Analysis. Part 3. Chemical Methods. SSSA Book Series: 5. WI, USA; 1996. pp. 1011–1069.
[23] D.L. Sparks, Environmental Soil Chemistry, 2nd edition, Academic Press, Amsterdam, 2003.
[24] M. Hosse, K.J. Wilkinson, Determination of electrophoretic mobilities and hydrodynamic radii of three humic substances as a function o pH and ionic strength, Environ. Sci. Technol. 35 (2001) 4301–4306.
[25] P. Attard, D. Antelmi, I. Larson, Comparison of the zeta potential with the diffuse layer potential from charge titration, Langmuir 16 (2000) 1542–1552.
[26] C.J. Milne, D.G. Kinniburgh, W.H. van Riemsdijk, E. Tipping, Generic NICA-Donnan model parameters for metal–ion binding by humic substances, Environ. Sci. Technol. 37 (2003) 958–971.
[27] D.G. Kinniburgh, W.H. van Riemsdijk, L.K. Koopal, M. Borkovec, M.F. Benedetti, M.J. Avena, Ion binding to natural organic matter: competition, heterogeneity, stoichiometry and thermodynamic consistency, Colloids Surf., A 151 (1999) 147–166.
[28] A. Majzik, E. Tombácz, Interaction between humic acid and montmorillonite in the presence of calcium ions II. Colloidal interactions: charge state, dispersing and/or aggregation of particles in suspension, Org. Geochem. 38 (2007) 1330–1340.
[29] L. Marang, S. Eidner, M. Kumke, M. Benedetti, P. Reiller, Spectroscopic characterization of the competitive binding of Eu(III), Ca(II) and Cu(II) to a sedimentary originated humic acid, Chem. Geol. 264 (2009) 154–161.
[30] W. Stumm, J.J. Morgan, Aquatic Chemistry. An Introduction Emphasizing Chemical Equilibria in Natural Waters, Wiley-Interscience, New York, 1970.
[31] N.A. Wall, G.R. Chopin, Humic acid coagulation: influence of divalent cations, Appl. Geochem. 18 (2003) 1573–1582.
[32] S. Hong, M. Elimelech, Chemical and physical aspects of natural organic matter (NOM) fouling of nanofiltration membranes, J. Membr. Sci. 132 (1997) 159–181.

[33] G. Chilom, J.A. Rice, Structural organization of humic acid in the solid state, Langmuir 25 (2009) 9012–9015.
[34] N. Janot, P.E. Reiller, X. Zheng, J.P. Croué, M.F. Benedetti, Characterization of humic acid reactivity modifications due to adsorption onto α-Al_2O_3, Water Res. 46 (2012) 731–740.
[35] J. Peuravuori, K. Pihlaja, Molecular size distribution and spectroscopic properties of aquatic humic substances, Anal. Chim. Acta 337 (1997) 133–149.
[36] S. Kang, B. Xing, Humic acid fractionation upon sequential adsorption onto goethite, Langmuir 24 (2008) 2525–2531.